Simulation of Volatility of Commercial Gasoline Based on Major Hydrocarbon Species

Younggy Shin*

(*Received March 26, 1997*)

Fuel volatility affects evaporative emissions and driveability. It is the property that must be changed with location and season. As exhaust gas emissions regulations become stringent, the margin of fuel injection schedule to allow for the variations of fuel volatility needs to be controlled tightly. It requires better understanding of fuel volatility effects on exhaust gas emissions and driveavility. Therefore, the modeling of fuel volatility is an essential basis for all theoretical approaches to address these issues. For the modeling, commercial gasolines were simplified with 13 major hydrocarbon species based on the carbon number and hydrocarbon families. Thermodynamic states of modeled fuels were calculated by the program SUPERTRAPP released by NIST (National Institute of Science and Technology). The program is based on the Peng-Robinson equation of state. The compositions of simulated fuels were calibrated with the specifications of commercial gasolnes such as ASTM distillation curve. Comparison with real fuels shows good agreement in front-end volatility represented by Reid vapor pressure and vapor-liquid ratios.

Key Words: Volatility, Gasoline, ASTM Distillation, Reid Vapor Pressure, Driveability, Vapor-Liquid Ratio, Mixture Preparation, Fuel Model, SI Engine

1. Introduction

Exhaust gas emissions regulations become more stringent for better air quality. For example, the ULEV (Ultra Low Emissions Vehicle) regulations to be effective from 1997 in California require to reduce hydrocarbon emissions (HC) to 50 % of the LEV (Low Emissions Vehicle) standard (0. 08 grams/mile) which is already tough to meet. Under this circumstance, the HC emissions emitted during starting and warm-up becomes more important. For example, the FTP (Federal Test Procedure) emissions test result of a prototype ULEV showed that the HCs from Bag 1 occupied 85% of the total HCs produced during the entire FTP-75 mode (Federal Test Procedure) emissions test (Horie et al., 1995). The high level of HC during engine starting and warm-up is attributed to poor mixture preparation resulting from cold engine condition. Under that condition, driveability issues also become critical. Therefore, understanding of fuel volatility is the first step to find possible ways for HC reduction and for driveability improvement. The understanding means plausible modeling of fuel volatility. A fuel volatility model is an essential basis on which any mixture preparation model can be built.

However, the modeling is quite challenging because gasoline is a mixture of more than 100 hydrocarbon species and the thermal environment of the intake port is transient and non-uniform. It is nearly impossible to model gasoline in detail by taking into account all of the hydrocarbon species. Chen et al. modeled fuel volatility by representing gasoline with 10 representative hydrocarbon species (Chen et al., 1994; Chen, 1996). The model was calibrated with the ASTM distillation curve and Reid vapor pressure (RVP). Chen et al.'s basic concept was adopted

* Sloan Automotive Laboratory, Massachusetts Institute of Technology, 77 Mass. Ave., Cambridge, MA 02139, U.S.A.

in this study and developed further to the extent of differentiating volatility of 28 types of commercial gasoline. The fuel modeling is a prerequisite for accurate modeling of the mixture preparation process. This paper describes the modeling procedure and shows comparison of the properties of real gasoline with the simulated fuels.

2. Equation of Thermodynamic State

In this study, gasoline, mixture of more than 100 hydrocarbon species, is simulated with 13 major species. To calculate thermodynamic properties of the simulated fuel, an equation of state should be known. For that purpose, the Peng-Robinson equation of state was applied (Peng and Robinson, 1976). Peng and Robinson proposed the following form of equation of state by taking into account the fact that in liquid phase mixtures the size of the hard sphere model for the molecules and the intermolecular attraction forces between different pairs of molecules are different:

$$P=\frac{RT}{v-b}-\frac{a(T)}{v(v+b)+b(v-b)} \tag{1}$$

where

$$a_{mix}=\sum_i\sum_j x_i x_j m_{ij} a_{ij} \tag{2}$$

$$b_{mix}=\sum_i x_i b_i \tag{3}$$

Constant a_{ij} and b_i in Eqs. (2) and (3) are functions of critical temperature T_c, critical pressure P_c and acentric factor w. Constant m_{ij} Eq.(2) is the binary interaction coefficient between component i and j. Fly and Huber developed a program called SUPERTRAPP to calculate the phase compositions of hydrocarbon mixtures based on the Peng-Robinson equation of state (Fly and Huber, 1992). It contains a database of 116 species, mostly hydrocarbons, and provides an option to calculate thermodynamic properties of a mixture either by the Peng-Robinson equation of state or by the NIST (National Institute of Standards and Technology) extended corresponding state model. The maximum number of constituents of a mixture which can be handled in SUPERTRAPP is 20. Thus, the number of constituents of any fuel model should not exceed 20.

3. Methodology for Formulating a Fuel Composition Model

Since the composition of real gasoline consists of more than 100 HC species, it should be simplified by small number of hydrocarbon species which could be good enough to differentiate volatility among commercial gasoline. Fuel volatility is classified by the following specifications: 1) ASTM distillation curves, 2) Reid vapor pressure, and 3) vapor-to-liquid ratios at specific temperatures. Their details will be described later. Although there is no specific rule to determine the number of species to simulate real gasoline, the following constraints are considered to determine the number. Plotting an ASTM distillation curve needs 9 data points and Reid vapor pressure needs one data point. The last specification (vapor-to-liquid ratios) are used to verify the validity of the fuel model by comparing vapor-to-liquid ratios. Therefore, the number of constraints to characterize fuel volatility is confined to 10. Although the volatility behavior is not linear to compositions of fuel constituents, the number of species of 10 or so might make sense. When it comes to the compositions of real fuels, they can be categorized in terms of carbon number and hydrocarbon family. To cover the low and high boiling ends of the ASTM curve, carbon numbers 4 and 13 had to be selected as lower and upper limits of a fuel model. In the same carbon number group, hydrocarbons are classified into three families due to different molecular structure (saturates (C_nH_{2n+2}), aromatics (C_nH_{2n-6}), and olefins (C_nH_{2n})). In general, saturates take 50 to 70% mass fraction of the total hydrocarbons, and aromatics 30 to 40 %, and olefins less than 10%. For simplicity of the modeling, olefins were excluded from the selection of representative species. Further subdivision was made to differentiate saturates and aromatics within a same carbon number group. To illustrate the formulation procedure, the methodology is applied to indolene as follows:

(1) Divide the fuel species into groups according

Table 1 Representation of indolene in major hydrocarbon species

Group	Molar ratio (%)	Mass (%)	Major species	Representative component	Molar ratio of representative component (%)
C4	9. 12	5. 47	n-butane	n-butane	8. 46
C5	14. 15	10. 48	2 M-butane	2 M-butane	8. 84
C6	8. 42	7. 46	23 dM-butane	23 dM-butane	2. 12
C6 r	2. 54	2. 05	benzene	benzene	2. 54
C7	8. 36	8. 64	23 dM-pentane	23 dM-pentane	3. 90
C7 r	17. 62	16. 77	toluene	toluene	17. 62
C8	23. 77	28. 05	224 tM-pentane	224 tM-pentane	8. 79
C8 r	2. 10	2. 30	m-zylene	m-zylene	0. 79
C9	1. 41	1. 87	225 tM-hexane	225 tM-hexane	0. 75
C9 r	6. 86	8. 51	124 tM-benzene	i-Propyl benzene	2. 42
C10	3. 76	5. 30	4 M-nonane	N-decane	0. 43
C11	1. 60	2. 57	C11 isoparaffins	n-undecane	0. 22
C12	0. 29	0. 53	C12 isoparaffins	n-dodecane	0. 02
total	100	100			56. 99

to their carbon number.

(2) For species with 6 and higher carbon numbers, the group is further subdivided into saturates and aromatics.

(3) The species with 4 or less carbon numbers and with 13 or more carbon numbers are grouped as one each.

(4) For each group, a major component which has the highest weight percent in each group is selected to represent the group.

Table 1 shows an example of the major-species fuel model for indolene. In the table, the first column shows the group identity (The number next to 'C' is carbon number and 'r' stands for aromatics). Column 2 and 3 are the sum of the molar and mass percentage of all species in a particular group. The actual weight percents of the major species in indolene are shown in column 5. Here, one problem associated with major species is that some particular major species are not listed among 116 compounds in the NIST program (SUPERTRAPP). Thus, those species had to be replaced with the species available in the NIST program which had similar properties. It was the case for the C9r, C10, C11 and C12 groups. Thus, the 124-tri-methyl benzene was represented by iso-propyl benzene, 4M-nomane by n-decane, C11

iso-paraffins by n-undecane, and C12 iso-paraffins by n-dodecane. The final representation is listed in the last column. The composition of the 13 representative components are adjusted so that the fuel model fits in with the ASTM distillation curve and the RVP of indolene. The adjustment is described in the next section.

4. Simulation of ASTM Distillation Test

The ASTM distillation curve is the most readily available information regarding fuel volatility. The major-component fuel model is used to simulate the ASTM distillation curve for different fuels. The ASTM distillation apparatus is shown in Fig. 1 (American Society of Testing Materials, 1992a). Fuel is distilled from the flask and the temperature is read by the thermometer as a function of the liquid condense collected. The functional relation constitutes the ASTM distillation curve. The process is not in equilibrium and there are significant thermal gradients within the apparatus. As described below, several important provisions have to be made to render an equilibrium flash calculation to represent the ASTM

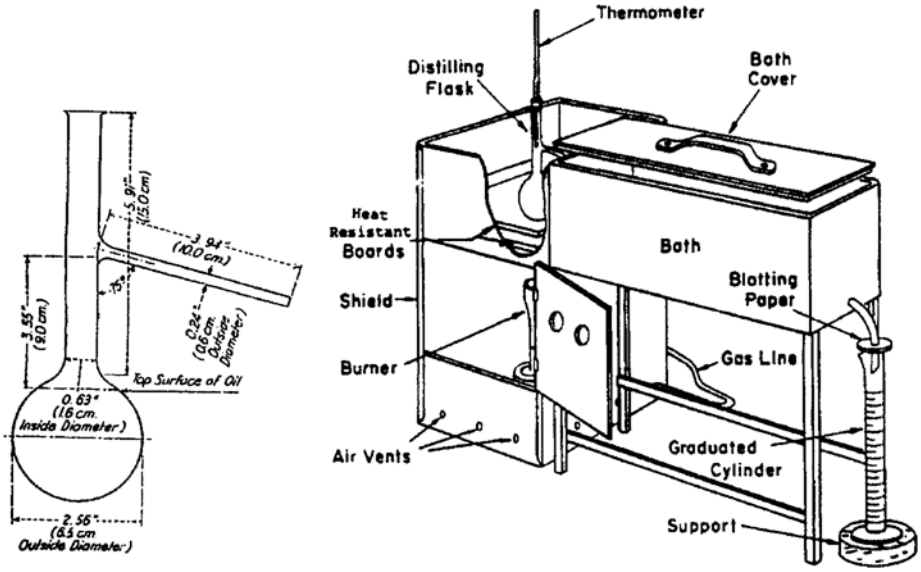

Fig. 1 ASTM distillation apparatus(D86-90)

distillation process.

To develop the method, the distillation process of a binary mixture of 50% isooctane and 50% n-pentane is simulated. The distillation data are shown as solid symbols in Fig. 2 (Obert, 1973). In that case, the species are well known and are well represented by the thermodynamic database of SUPERTRAPP. Therefore, the only unknown is the manner of the process simulation.

Considering the boiling points of the two components (n-butane: 309K, isooctane: 372K), it is clear that the initial and end boiling points of the distillation curve agree with the boiling points of isooctane and n-butane. It means that the lightest component starts to boil off at its boiling temperature and finally the heaviest one boils off at its boiling temperature at the end boiling point of the curve where only the heavier component exists. Therefore the ASTM curve simulation program should be able to simulate the behavior. When the presence of no air is assumed in thermodynamic equilibrium, the simulation result predicts the higher initial boiling point than the data as shown in Fig. 2. It is due to the presence of the heavier component, isooctane. It is well known that the presence of air greatly facilitates gasoline evaporation (Coordinate Research Council

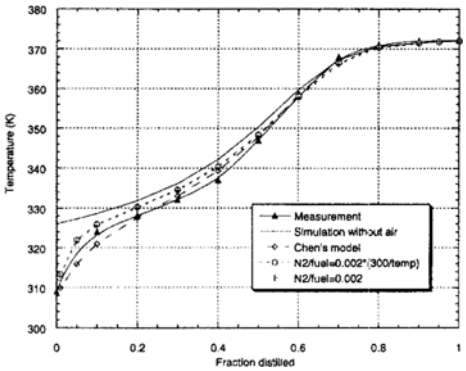

Fig. 2 ASTM distillation curves for iso-octane/n-pentane mixture(50/50)

Handbook, 1946). Therefore the ASTM curve simulation model should include air in the mixture to lower the initial boiling point. Another point to note is that the end boiling point of the curve is close to the boiling point of the heavier component, isooctane. To account for distillation behavior, Chen et al. decreased the amount of nitrogen linearly between the initial boiling point and the end point (Chen, Cheng, and DeWitte, 1994). Here the use of nitrogen instead of air was for the convenience of the simulation. Since the interactions between nitrogen and air with hydrocarbons are essentially the same, the use of nitro-

gen in place of air should not make any difference. The results of the simulation in the presence of nitrogen are shown as open-rhombus symbols in Fig. 2. The simulation is in good agreement with the simulation data.

Although Chen et al.'s idea shows good agreement with the data, it lacks physical interpretation of the mass transfer process within the flask from the following reason. Furthermore, the initial nitrogen ratio of 0.005 was found to be too high as will be explained later in the section of the Reid vapor pressure. There should always exist air in the flask during the whole distillation process to make possible mass transfer by diffusion between air and the hydrocarbons vapor. The author assumes two cases. One is the presence of nitrogen at a fixed molar fraction of the remaining hydrocarbons in liquid phase. In that case, the effect of the fixed molar ratio on the distillation behavior is more pronounced near the initial boiling point than near the end point. It is because near the end point only the heavier component remains in the flask and it boils off as soon as the temperature reaches its boiling temperature regardless of the presence of nitrogen. The ratio of 0.002 is found to show good agreement both in the ASTM distillation curve and in the Reid vapor pressure. The case of the fixed ratio is shown as cross symbols in Fig. 2. It also shows good agreement with the data. The other idea is to take into account temperature effect on the molar ratio of nitrogen. The nitrogen density in the flask decreases as the temperature of the liquid hydrocarbon increases. Therefore, by scaling the ratio of nitrogen with the nitrogen density, the ratio can be expressed as follows:

$$\frac{N_{N_2}}{N_{remaining\ fuel}} = \left(\frac{N_{N_2}}{N_{fuelinput}}\right)_{I.B.P} \frac{300}{T(K)} \quad (4)$$

The case of varying nitrogen density is shown as open-circle symbols in Fig. 2. This case shows exactly the same curve as that with the fixed ratio of nitrogen. It indicates that the consideration of varying nitrogen density according to the distillation temperature is not important. Chen et al.'s curve deviates from the other two simulation cases. It is because they used 0.005 of the initial molar ratio of nitrogen instead of 0.002. The use of 0.005 was found to underestimate the composition of lighter hydrocarbon components, leading to lower Reid vapor pressure than the test data as will be shown in Fig. 6.

Table 2 Composition of SYNGAS

Component	Mass(%)	Mole(%)
n-Pentane	20	23. 9
i-Pentane	20	23. 9
Cyclopentane	5	6. 2
1−Hexane	5	5. 2
Toluene	18	16. 9
Toluene	18	16. 9
n-Octane	5	3. 8
i-Octane	20	15. 1
i-Propylbenzene	7	5. 0

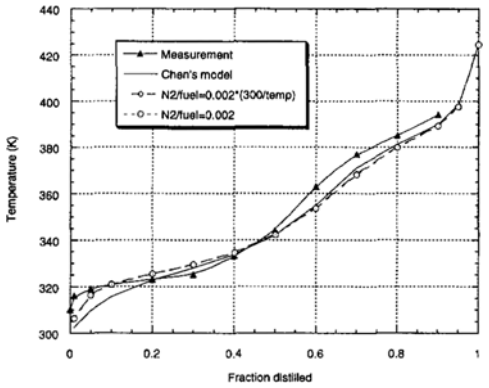

Fig. 3 ASTM distillation curves for SYNGAS

The above three simulation models were compared in a multi-component fuel of a known composition. Reddy made an eight-component fuel named 'SYNGAS' and measured the ASTM distillation curve and the Reid vapor pressure (Reddy, 1986). Table 2 shows the composition of SYNGAS.

Since the thermodynamic data for all the components are available in the NIST data base, the major-fuel component model is an exact representation of the fuel. The results are shown in Fig. 3. The calculated values show good agreement with the test data. As indicated above, Chen's model predicts lower distillation temperatures at the initial stage of the distillation because of its

higher molar ratio of nitrogen (0.005). The good agreement gives confidence in the simulation procedure.

5. Reid Vapor Pressure

An engine is said to be vapor locked when either partial or complete interruption occurs in the liquid fuel flow because of vaporization of the fuel. The vapor will occupy a greater volume than the liquid and therefore the amount of fuel flow will be reduced. The reduction will cause either a loss in power or else complete stoppage of the engine. The vapor-lock tendencies of gasoline are directly related to the front-end volatility (mass fraction distilled from 0 to 50 %) (Obert, 1973). RVP is one of the measures to evaluate vapor-lock tendencies. The RVP test procedure is standardized by ASTM (American Society for Testing Materials, 1992b): liquid fuel at 0 °C is connected to a chamber filled with air at 37.8 °C and four times the fuel volume. The equilibrated pressure of the air-fuel mixture at constant volume and at constant temperature of 37.8 °C is calculated. The vapor pressure for specific gasoline is largely determined by its individual compositions. The fuels with higher vapor pressure display a greater tendency to vaporize and form vapor locks thus impairing operation at higher temperatures. Since RVP is measured under the thermodynamic equilibrium condition, the major-component fuel model should show good agreement with the data to confirm its validity. The fuel model are tested with SYNGAS. Since its composition is known and the components are available from the database of SUPERTRAPP, the calculation of RVP is straightforward. The result is 0.638 bar whereas the measured value is 0.686 bar (Reddy, 1986). Although they are not exactly the same, the difference is tolerable in that a typical variation among the measured RVP as will be shown in Fig. 6 is about 0.05 bar, and it could be interpreted as the accuracy limit of SUPERTRAPP.

6. Application of the Major-Component Fuel Model to Commercial Gasoline

The methodology of the major-component fuel model is established as follows:

(1) A practical fuel is modeled with 13 major species. Depending on the end boiling point, either of n-dodecane (C12) or n-tridecane (C13) is chosen as the heaviest component.

(2) The composition of the individual components is calibrated by comparing the calculated ASTM distillation curve with the measured ASTM distillation curve of the test fuel. The simulation of the ASTM distillation curve is based on the assumption of the fixed molar ratio (=0.002) of nitrogen to liquid fuel.

(3) RVP is calculated using the calibrated composition of the major components and compared with a measured value. Until the difference becomes minimal, the composition of lighter components is adjusted while maintaining good agreement between the simulated ASTM distillation curve and the measured one. RVP is found to be very sensitive to the composition of lighter components.

To test the major-component fuel model, the following fuel matrix is used as reference data. The specifications of the fuel matrix were provided by Chrysler Corporation (Private communication, 1997). The gasolines were sampled all over the united states. They represent the whole range of possible variations of fuel volatility. Therefore, simulated fuel models can be used to investigate the fuel effects on mixture preparation behavior during starting and warm-up. The fuel simulation is conducted by comparing the ASTM distillation curve and RVP. Figure. 4 shows an example of comparison between a real fuel and the corresponding simulated fuel. It shows good agreement between the two fuels.

Calibration of simulated fuel compositions was repeated over the whole fuel matrix. The calibration procedure by trials and errors continued until a simulated fuel composition led to good agreement between a measured distillation curve

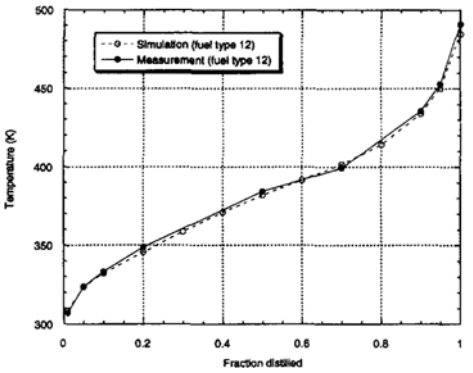

Fig. 4 Comparison of ASTM distillation curve between gasoline and corresponding fuel model

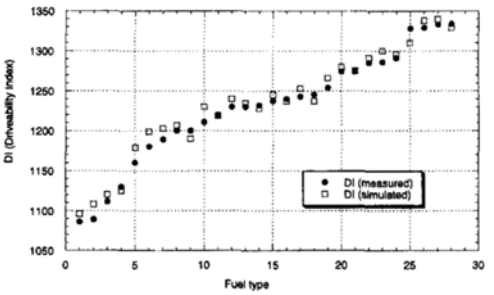

Fig. 5 Comparison of Driveability Index between commercial gasolines and corresponding simulated fuels

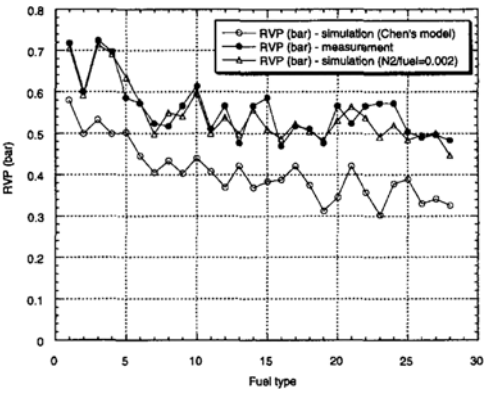

Fig. 6 Comparison of RVP between data and simulation results

and a simulated distillation curve. Since all of the 28 distillation curves can not be shown in this paper, their comparison was substituted with the comparison of DI (Driveability Index). DI is a measure of evaluating fuel volatility effect on vehicle driveability especially during warm-up. It is defined as follows:

$$DI = 1.5 \times T_{10} + 3 \times T_{50} + T_{90} \qquad (5)$$

where T_{10}, T_{50} and T_{90} are the distillation temperatures corresponding to mass fraction distilled 0.1, 0.5 and 0.9, respectively. DI is calculated based on either Fahrenheit degree (°F) or Celsius degree (°C) Since DI based on Fahrenheit degree is more often used by convention, it will be applied in this paper. Figure 5 shows the comparison of DI between real fuels and simulated fuels. The good agreement is the result of calibration efforts. Now it should be checked if the simulated fuel models display good agreement with other fuel properties.

7. Comparison of Reid Vapor Pressure

RVP is used as one of the measures to evaluate the tendencies to form vapor locks. The vapor-to-liquid (V/L) ratio under RVP test procedure is 4. However, it is too small compared to the V/L ratio which can be tolerated by the automotive system without vapor locks. Because of the small V/L ratio under RVP test procedure, it is very sensitive to the composition of very light hydrocarbons. Figure 6 shows the comparison of RVP between the data and the simulation results. To address the importance of the composition of lighter components in determining RVP, the simulated RVP based on Chen's simulation model of ASTM distillation process was compared. The RVP based on Chen's model shows lower values shifted from the measured RVP by 0.1 bar or so. It was caused by assuming too large molar ratio of nitrogen to liquid fuel which was 0.005. Larger molar ratio of nitrogen facilitated evaporation of heavier hydrocarbons components, resulting in allocation of smaller molar fractions of lighter hydrocarbon components during the fuel simulation process. On the other hand, the fixed molar ratio of nitrogen to liquid fuel of 0.002 led to good agreement between the simulation and the measurement. It indicates that the molar ratio

of 0.002 is a good approximation to simulate the composition of light components.

8. Comparison of V/L Ratios

High V/L (vapor-to-liquid) ratios tend to form vapor locks. Thus, high V/L ratios should be avoided. There are temperatures at V/L of 4, 10, 20, 45, etc. In particular, the temperature at V/L of 20 is used to predict performance of excessively volatile gasoline. As opposed to excessively low volatility (high driveability index) which leads to poor evaporation, fuel with a temperature at V/L of 20 which is too low may begin to generate significant vapor upstream of the fuel injector or carburetor. Thus, the fuel doesn't get to the injector as a liquid and there will be extreme lean excursions, leading to hot restart driveability problems. In fact, the temperature at V/L of 20 is often referred to as the vapor lock index. U. S. gasoline specifications for the temperature at V/L of 20 allow for five classes, ranging from not greater than 40.5 °C in the north in the winter, to not greater than 60 °C in the summer.

The test procedure to measure V/L ratios are specified by ASTM (American Society for Testing Materials, 1994a). In the procedure, the vapor-liquid ratio burette containing fuel only is immersed into the water bath whose temperature is precisely controlled. The fuel is sealed off with either glycerol or mercury to prevent air from getting in. The V/L according to the water bath temperature is read from the scale on the burette. Since the measurements are made under thermodynamic equilibrium, the data can be directly applied to verify the fuel simulation program. The V/L data were available from the fuel specifications provided by Chrysler Corporation (Private communication, 1997). The comparisons of temperatures at different V/L are shown in Fig. 7. The temperatures at V/L of 4 show good agreement between the data and the simulation. As the V/L ratio increases, the temperature difference between the data and the simulation also increases up to 5~7 °C at V/L of 45. The investigation of the discrepancy may elucidate the limitations of the fuel model. Since it is not easy to

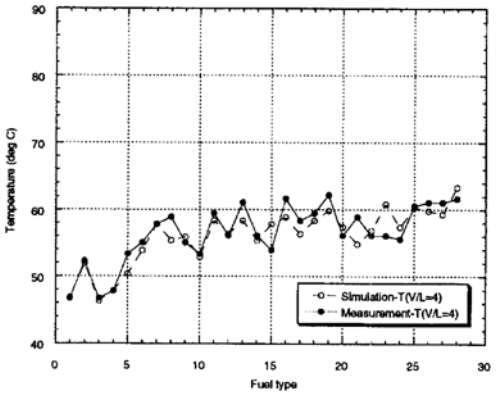

(a) V/L=4

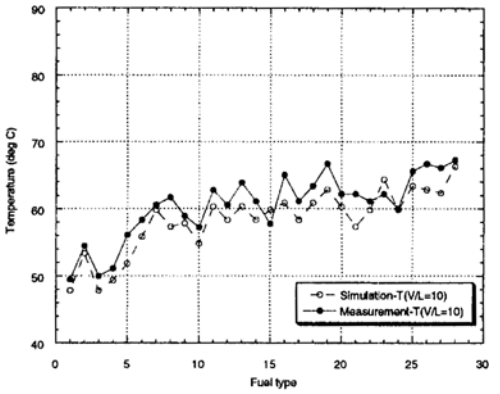

(b) V/L=10

Fig. 7 Comparison of V/L rations between data and simulation results

measure the V/L ratios according to the ASTM procedure, as an alternative, ASTM provided the following linear equation to estimate the values in terms of ASTM distillation data and RVP (American Society for Testing Materials, 1994b).

$$T_{V/L=20} = 52.47 - 0.33RVP + 0.2T_{10} + 0.17T_{50} \quad (6)$$

where:

$T_{V/L}$ = temperature, °C, at V/L of 20:1
RVP = Reid vapor pressure, kPa
T_{10} = distillation temperature, °C, at 10% evaporated, and
T_{50} = distillation temperature, °C, at 50% evaporated.

The temperatures estimated by the ASTM linear method are quite close to the test data as

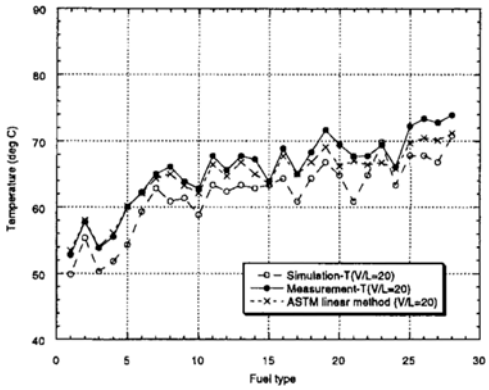

(c) V/L=20

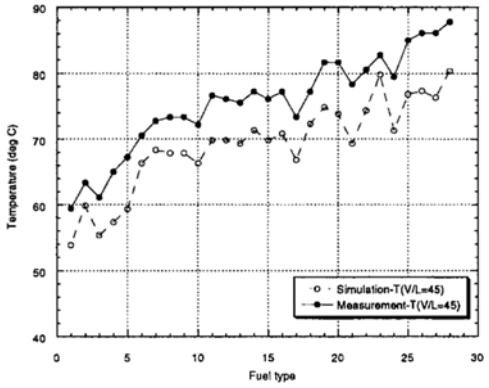

(d) V/L=45

Fig. 7 Comparison of V/L rations between data and simulation results

shown in Fig. 7(c). According to Fig. 6, RVP data are in such good agreement with the simulation results that the discrepancy in RVP doesn't lead to the temperature difference by 2~3 ℃ at V/L of 20. Thus, the discrepancy between the simulated fuels and the real fuels may be attributed to errors in predicting T_{10} and T_{50} by about 5 ℃ each. However, if the fuel composition is adjusted so that the simulated distillation temperatures are increased by 5℃, it will end up with significant deviation of the simulated RVP from the measured RVP, which would make worse the prediction of the temperature at V/L of 20. In conclusion, it is a limitation of the fuel model caused by representation of real fuel with limited number of hydrocarbon species. In spite of the limitation, the fuel model is useful in predicting

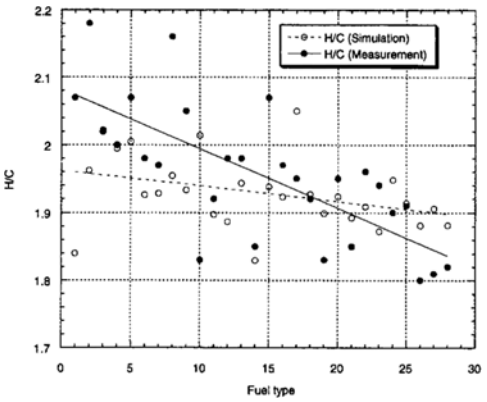

Fig. 8 Comparison of H/C between data and simulation results

front-end volatility responsible for the mixture preparation and driveability during warm-up because the temperature difference by 2~3℃ is not significant.

9. Other Comparisons

For further comparison with real fuels, the ratio of the number of hydrogen atoms to the number of carbons, H/C, was investigated. Fig. 8 shows the comparison. Linear regression of H/C results in two different slopes. The simulated one is smoother. It is because the major-component model can not fully represent the compositions of real fuels. In that model, the species consist of saturates (C_nH_{2n+2}) and aromatics (C_nH_{2n-6}). The aromatics are taken into account from only carbon number 6 to 9. The rest species from carbon number 4 to 13 are all saturates. When it comes to real fuels, there also exist olefins (C_nH_{2n}) which constitute less than 10% of the mass fraction of the hydrocarbons in the fuels. Thus, the smoother slope in simulated fuels is attributed to the existence of the saturates as dominant species than expected in the real fuels. It is evidenced in Fig. 9 (a) and (b). The comparison in Fig. 9 (a) reveals that the saturates in the simulated fuels have more mass fractions than in the real fuels. In the case of Fig. 9 (b), the aromatics tend to show similar proportions in the simulated fuels and the real fuels although their slopes of linear regression are different. There-

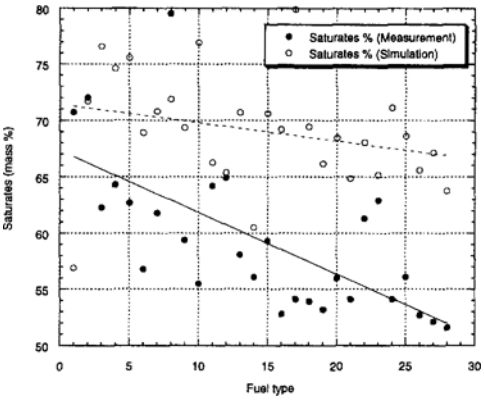

(a) Saturates contents

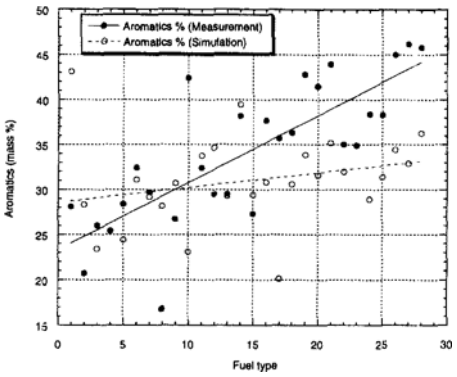

(b) Aromatics contents

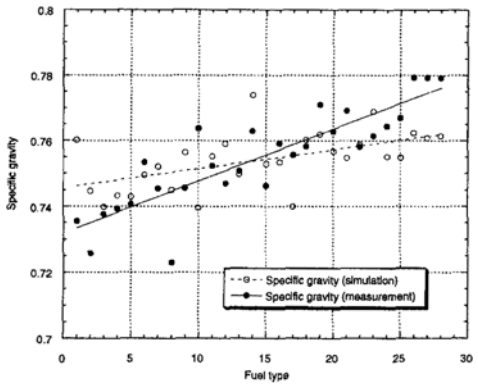

(c) Specific gravity

Fig. 9 Comparisons between data and simulation results

fore, the difference in the mass fraction of the saturates between the simulated fuels and the real fuels is attributed to the unmodelled olefins. The unmodelled olefins were incorporated into the saturates in the simulation process. Although it was not intended, the calibration process of the simulated fuels with the ASTM distillation curves and RVP resulted in the incorporation of the olefins into the aromatics. Therefore, if more components than those considered in this study are included in the fuel model, it is expected that the simulated fuels will show closer resemblance with the real fuels. Figure. 9 (c) shows the comparison of specific gravity. The increasing tendency of specific gravity with the fuel type number increased is due to the increasing proportions of heavy hydrocarbon components which are difficult to evaporate and hence resulting in high DI as shown in Fig. 5.

10. Application to Oxygenated Fuels

Oxygenates such as alcohols and MTBE (methyl tertiary butyl ether, $C_4H_9OCH_3$) are added to hydrocarbon fractions function in two ways. Firstly they have high blending octane, and so can replace high octane aromatics in the fuel. These aromatics are responsible for disproportionate amounts of CO and HC exhaust emissions. This is called the "aromatic substitution effect". Oxygenates also cause engine without sophisticated engine management systems to move to the lean side of stoichiometry, thus reducing emissions of CO (2% oxygen can reduce CO by 16%) and HC (2% oxygen can reduce HC by 10%) (Piel and Thomas, 1990), and other researchers have observed similar reductions also occur when oxygenates were added to reformulated gasoline on older and newer vehicles, but have shown that Nox levels might increase, as also may some regulated toxins (Auto/Oil Air Quality Improvement Research Program, 1991a, 1991b)

Considering the increasing importance of oxygenates, it is worthwhile to model oxygenated fuels. One problem with the modeling is that the database of oxygenates is not available in SUPERTRAPP, but it allows to add more components to the database. Since it is beyond the scope of this work to find the binary interaction coefficients between component i and j in Eq. (2),

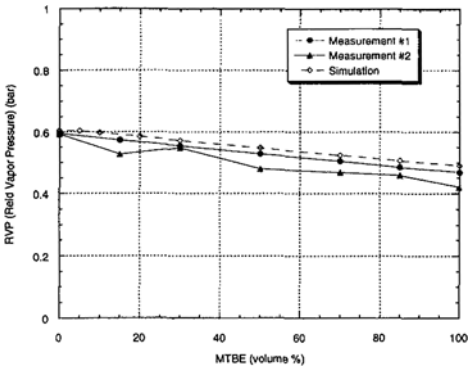

(a) MTBE blended fuels

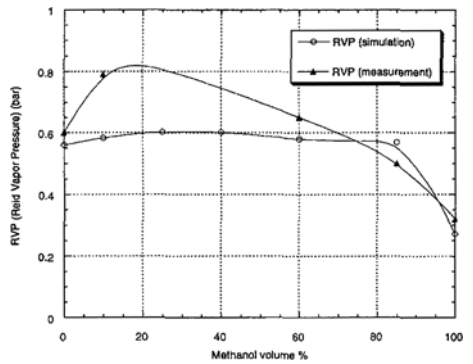

(b) Methanol blended fuels

Fig. 10 Comparison of RVP

m_{ij}, the coefficient is simply assumed as unity. The physical model of the Peng-Robinson equation of state for the species interaction is based on non-polar compounds which are good approximation to the hydrocarbons. Because of the nature of the polar / non-polar interaction which is very different from the non-polar / non-polar interaction, the assumption of unity interaction coefficient may lead to errors, especially in the case of methanol which is highly polar.

The fuel simulation model is applied to MTBE-blended gasoline. Figure. 10 (a) shows the comparison of RVP between the simulated fuels and the real fuels. Relatively good agreement is noticed. Thus, it is viable to assume the binary interaction coefficient as unity for MTBE. On the other hand, the comparison in the case of methanol-blended fuels, as shown in Fig. 10 (b), reveals a significant difference, especially when the methanol content is small. The difference resulted from the ability of methanol to form very volatile azeotropes that cause the fuel's vapor pressure to increase. The tendency to form azeotropes are pronounced significantly at low methanol contents. Therefore, it is not appropriate to model the methanol-blended fuels with the fuel simulation model by assuming the binary interaction coefficient as unity for methanol.

11. Conclusions

Volatility of commercial gasoline was simulated with 13 representative hydrocarbon species. Thermodynamic states of the simulated fuel consisting of the 13 species were calculated by the Peng-Robinson equation of state. The compositions of the representative species were calibrated with the ASTM distillation curve and Reid vapor pressure. The simulated fuel shows good agreement with vapor-liquid ratios of 4 and 10. The discrepancy observed in vapor-liquid ratios of 20 and 45 reveals the limitation of the fuel model. The limitation is inevitable because gasoline is represented by 13 hydrocarbon species. However, the errors in the temperatures at V/L of 20 are moderate enough for the fuel model to be used to predict the front-end volatility. The front-end volatility is responsible for the mixture preparation and driveability during warm-up. According to the comparison with respect to the composition of hydrocarbon families, the simulated fuel shows good fit with the real fuel within its limitations such as limited number of hydrocarbons. Therefore, as far as the composition of the simulated fuel is calibrated with the ASTM distillation data and RVP, the simulated fuel is accurate enough to predict the front-end volatility and it can be used as a test fuel to drive any mixture preparation model. When it comes to oxygenated fuels, the fuel model shows good agreement with MTBE-blended fuel, but not with methanol-blended fuel. To simulate the methanol-blended fuel, the binary interaction coefficients with the methanol should be determined from experiments.

References

American Society of Testing Materials, 1992a, *Standard Test Method for Distillation of Petroleum Products,* Designation: D86-90, Annual Book of ASTM Standards, Vol. 05. 03.

American Society of Testing Materials, 1992b, *Standard Test Method for Vapor Pressure of Petroleum Products (Reid Method),* Designation D323-90, Annual Book of ASTM Standards, Vol. 05. 01.

American Society of Testing Materials, 1994a, *Standard Test Method for Vapor-Liquid Ratio of Spark-Ignition Engine Fuels,* Designation: D2533-93a, Annual Book of ASTM Standards.

American Society of Testing Materials, 1994b, *Standard Test Method for Vapor-Liquid Ratio of Spark-Ignition Engine Fuels,* Designation: D2533-93a, Annual Book of ASTM Standards.

Auto/Oil Air Quality Improvement Research Program, 1991a, "Mass Exhaust Emissions Results from Reformulated Gasoline," *Technical Bulletin* No. 4 (May).

Auto/Oil Air Quality Improvement Research Program, 1991b, "Exhaust Emissions of Toxic Air Pollutants Using RFGs," *Technical Bulletin* No. 5.

Chen, K. C., 1996, *Fuel Effects on Driveability and Hydrocarbon Emissions of Spark-Ignition Engines During Starting and Warm-up Processes,* Ph. D. Thesis, Dept. of mechanical Engineering, M. I. T. .

Chen, K. C., DeWitte, K., and Cheng, W. K., 1994, "A Species-Based Multi-Component Volatility Model for Gasoline," *SAE paper* 941877.

Coordinate Research Council Handbook, 1946, p. 236.

Horie, K., Takahashi, H., and Akazaki, S., 1995, "Emissions Reduction During Warm-Up Period by Incorporating a Wall-Wetting Fuel Model on the Fuel Injection Strategy During Engine Starting," *SAE paper* 952478.

Fly, J. F. and Huber, M. L., 1992, "IST Thermophysical Properties of Hydrocarbon Mixtures Database (SUPERTRAPP)," National Institute of Standards and Technology Standard Reference Data Base 4 - Version 1. 0, Gaithersburg, MD 20899, July.

Obert, E. F., 1973, "Internal Combustion Engines and Air Pollution," p. 256.

Peng, D. Y. and Robinson, D. B., 1976, "A New Two-Constant Equation of State," I&EC Fund., 15, 59~64.

Piel, W. J. and Thomas, R. X., 1990, "Oxygenates for Reformulated Gasoline," *Hydrocarbon Processing*, p. 68~73.

Private communication with Chrysler Corporation, 1997, *Properties of 28 Types of Commercial Gasoline in U. S. A.,* Chrysler Corporation.

Reddy, S. R., 1986, "Evaporative Emissions from Gasolines and Alcohol-Containing Gasolines with Closely Matched Volatilities," *SAE paper* 861556.